Colloids and Surfaces A: Physicochem. Eng. Aspects 468 (2015) 40–48

Contents lists available at ScienceDirect

Colloids and Surfaces A: Physicochemical and Engineering Aspects

journal homepage: www.elsevier.com/locate/colsurfa

Self-organization and solubilization in binary systems based on hyperbranched polyesters polyols

Marianna P. Kutyreva[a,*], Arthur A. Khannanov[a], Lucia Ya. Zakharova[b,c,**], Nikolay A. Ulakhovich[a], Gennadiy A. Kutyrev[c], Dinar R. Gabdrakhmanov[b,c]

[a] Kazan Federal University, 18, st. Kremlyovskaya, Kazan 420008, Russian Federation
[b] A.E. Arbuzov Institute of Organic and Physical Chemistry of Kazan Scientific Center of Russian Academy of Sciences, 8, st. Arbuzov, Kazan 420088, Russian Federation
[c] Kazan National Research Technological University, 68, st. K. Marx, Kazan 420015, Russian Federation

HIGHLIGHTS

- Research the structure of mixed micelles in binary systems Boltorn H/surfactant.
- Investigate the self-organization of binary systems Boltorn H/non-ionic surfactant.
- Investigate Orange OT solubilization by mixed micelles Boltorn H/surfactant.
- The influence of surfactants on self-organization of the Boltorn H structure.

GRAPHICAL ABSTRACT

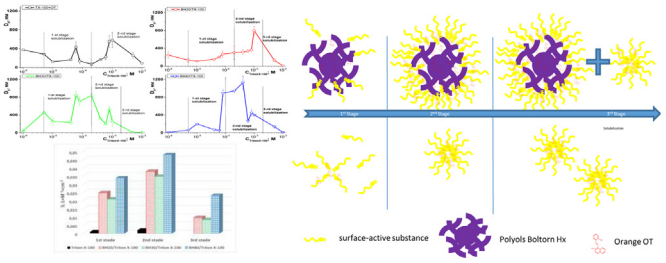

ARTICLE INFO

Article history:
Received 8 September 2014
Received in revised form
27 November 2014
Accepted 30 November 2014
Available online 10 December 2014

Keywords:
Hyperbranched polyester polyols Boltorn H*x*
Polymer surfactant system
Binary systems
Self-organization
Solubilization

ABSTRACT

The work includes the determination of relationships of the solubilization process of biodegradable hyperbranched polyester polyols Boltorn H*x* of second, third and fourth generation by nonionic surfactants (TX-100, Brij-35, Tween-20). The impact of hyperbranched polyester polyols in binary systems Boltorn H*x*/surfactant on surface-active properties of surfactants, dimensions of assemblies and solubilization capacity has been estimated with respect to Orange OT dye. It has been shown that solubilization capacity rises by an order of magnitude in binary system Boltorn H*x*/TX-100 and decreases in binary system Boltorn H*x*/Tween-20.

1. Introduction

The polymers self-organization effect presents a profound theoretical interest in the field of obtaining materials with various composition, shape, structure and properties. Polymeric assemblies can have various applications: honeycomb structure models, biosensors, encapsulating agents for drug delivery and effective patterns for controlled construction of functional materials [1–4].

* Corresponding author. Tel.: +7 432 337 165; fax: +7 432 337 416.
** Corresponding author at: A.E. Arbuzov Institute of Organic and Physical Chemistry of Kazan Scientific Center of Russian Academy of Sciences, 8, st. Arbuzov, Kazan 420088, Russian Federation. Tel.: +7 843 272 1684; fax: +7 843 236 7542.
E-mail addresses: mkutyreva@mail.ru (M.P. Kutyreva), lucia@iopc.ru (L.Ya. Zakharova).

http://dx.doi.org/10.1016/j.colsurfa.2014.11.058
0927-7757/

Provision of controlled capture and release of a target component by a polymer is only possible if they are sensitive to external influences, e.g. pH and temperature [5]. In this respect, pH is one of the most commonly used functional parameter of these supramolecular systems.

Linear polymers, block copolymers [6–10], hyperbranched polymers [7,11–13] and dendrimers [14] are successfully used in the creation of such self-organizing systems. Among these polymer types, hyperbranched polymers and dendrimers present a number of benefits for the performance of the abovementioned tasks [15]: they have an irregular structure, and can be easily synthesized in a one step with a high level of yield. Moreover, hyperbranched polymers are low-toxic, biodegradable, they can be easily modified and synthesized, what makes them highly suitable for drug delivery. The most important hyperbranched polymers today are hyperbranched polyester polyols (HPP) [15–18]. A number of research works have demonstrated the possibility of their use as self-organizing systems [19–22]. However, the research works mostly describe the self-assembly process of modified hyperbranched polymers [7,11–13,23,24]. For instance, the authors of work [25] have investigated the self-association of Boltorn H40 modified by succinyl oxide in water solutions. The pH dependency of the association has been studied using the methods of AFM investigation, dynamic and static light scattering of water solutions with various pH values. The majority of research works on this topic has been performed with the use organic solvents [25,26]. However, self-organization of non-toxic biodegradable unmodified HPP in water solutions is practically unexplored. This is particularly important for the development of self-organizing systems on the basis of HPP for biomedical applications including medical delivery systems. Variation of a polymer's solubility by means of a complex chemical modification can lead to an increase of the polymer's toxicity.

The issue could be solved by the creation of binary systems polymer/surfactant combining of micellar delivery systems and hard covalent bonding of the substrate [12,13,22,27,28]. Besides, in a number of cases synergistic effect can be achieved by means of surfactant and polymer selection. Similar identified binary systems are based on linear polymers, such as: PEI_{25}, PEI_{50}, PVP, PTFE, PMMA, PEG [29–37]. New systems HPP/surfactant can potentially be used for medical delivery to organs and cells.

Thus, the purpose of this work is the creation of a method for HPP dissolution using non-toxic surfactants and the definition of patterns determining the self-assembly and solubilization process in binary systems HPP/surfactant.

2. Experimental

2.1. Materials

2.1.1. Hyperbranched polymers

The following Boltorn H*x* commercial hyperbranched polyester polyols were used in this work: Boltorn H20 (**1**), Boltorn H30 (**2**), Boltorn H40 (**3**) of second, third and fourth generation (Fig. 1), respectively, synthesized on the basis of AB_2-type monomer of 2,2-dihydroxy-methylpropene acid with ethoxylated pentaerythritol as the ring (Polymer Factory Sweden AB, Teknikringen 48 Stockholm, Sweden, SE-114 28). Boltorn H20 contains 16 hydroxyl groups, Mr = 1749.8 g/mol with hydroxyl value 212.5 mg KOH/g (Fig. 1a), Boltorn H30 contains 32 hydroxyl groups, Mr = 3608 g/mol with hydroxyl value 480–520 mg KOH/g (Fig. 1b). Boltorn H40 contains 64 hydroxyl groups, Mr = 7323 g/mol with hydroxyl value ~740 mg KOH/g (Fig. 1c).

2.1.2. Surfactants and dyes

The following commercial surfactants were used in this work: Brij-35 (Uniqema Americas LLC, Mr = 1119 g/mol, CMC = 1.7×10^{-4} mol/l, T_{melt} = 38 °C), Triton-X100 (Sigma–Aldrich GmbH Mr = 625 g/mol, CMC = 2×10^{-4}, T_{boil} = 65 °C) и Tween-20 (Sigma–Aldrich GmbH Mr = 1228 g/mol, CMC = 2×10^{-5}, T_{boil} = 65 °C) without additional purification. Solubilization capacity was studied using 1-(o-tolylazo)-2-naphthol (Orange OT) Sigma–Aldrich GmbH, CAS Number 2646-17-5, molar extinction coefficient of water solutions of the surfactant is 17,400 L M^{-1} cm^{-1}.

2.2. Methods

2.2.1. Preparation of the polymer

Initially, Boltorn H*x* (*x* = 20, 30, 40) polyester polyols were heated to 140 °C and extracted by vacuum water vapour in order to disrupt the hydrogen bond network [37]. Then HPP was dissolved in acetone and deposited using dehydrated diethyl ester with consequent vacuum drying at pressure 1×10^{-2} mm Hg. The obtained white sediment was ground into monosize powder using an agate mortar.

2.2.2. Preparation of test solutions

Boltorn H*x* (*x* = 20, 30, 40) polyester polyols solutions were prepared by dissolution of accurately weighed portions of the required concentration of HPP prepared in a surfactant solution, and used within 24 h. Before studying, target substance solutions were subjected to ultrasonic material dispersion. The original surfactant solutions with concentration above the CMC point were prepared by dissolution of their accurately weighed portions in double-distilled water, subjected to ultrasonic material dispersion and used for the preparation of solutions with specified concentration. The research was performed at 25 ± 0.1 °C.

2.2.3. Surface tension measurements

Surface tension measurements were performed using the du Nouy ring detachment methods with the tensiometer K6 (Kruss). Each data point represented the average of ca. 15 measurements of surface tension. Each concentration dependence was obtained three times and results were within 2%.

2.2.4. Solubilization of Orange OT

Orange OT was used as received. The solubilization experiments were performed by adding an excess of crystalline dye to solutions. These solutions were allowed to equilibrate for about 48 h at room temperature. They were filtered and their absorbency was measured at 505 nm (molar extinction coefficient 17,400 L M^{-1} cm^{-1}). Electronic absorption spectra were taken on a Lambda 750 (PerkinElmer) spectrophotometer in the wavelength range 190–900 nm at a temperature of 25 ± 0.01 °C with the usage of a thermostating system including a thermostated cuvette holder a Julabo MB 5A flow thermostat and a Peltier RTR1 thermostat. Quartz cuvettes with a thickness of 1 cm were used in measurements.

2.2.5. Dynamic light scattering measurements

Dynamic light scattering (DLS) measurements were performed by means of Malvern Instrument Zetasizer Nano. The Malvern DTS software and the second-order cumulant expansion methods analysed the measured autocorrelation functions. The effective hydrodynamic radius (RH) was calculated according to the Stokes–Einstein relation: DS = *kBT*/6*pg* RH, in which DS is the diffusion coefficient, where *kB* is the Boltzmann constant, *T* is the absolute temperature and *g* is the viscosity.

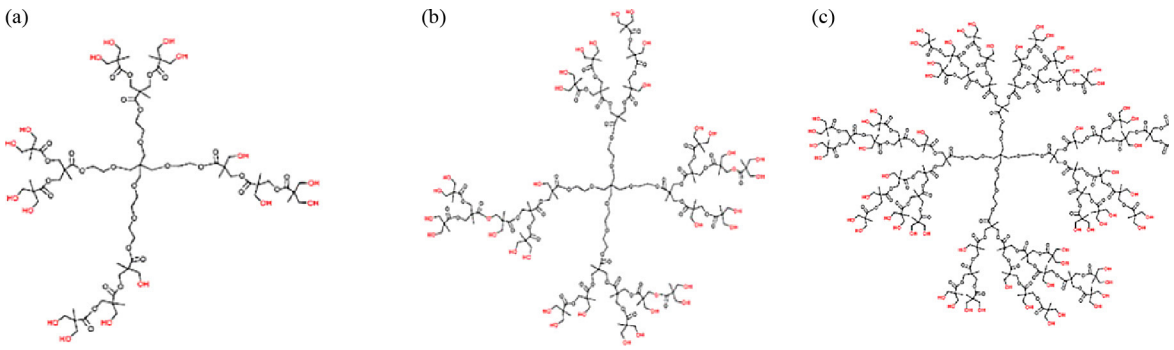

Fig. 1. Idealized structures of Boltorn H20 (1a), Boltorn H30 (1b), Boltorn H40 (1c) HPP.

2.2.6. Measurements of pH

Measurements of pH were taken at 25 ± 0.05 °C on a pH metre Hanna with combined pH electrode HI 1330 ("Hanna Instruments" Germany) with the accuracy of ±0.1 pH units.

2.2.7. Measurements of conductivity

Conductivity was estimated on Conductometer WTW InoLab Cond 720.

3. Results and discussions

Hyperbranched polyester polyols series Boltorn H*x* (*x* = 20, 30, 40) (Fig. 1) are practically insoluble in water. Solubility decreases with the rise of polymer generation.

The following non-ionic surfactants were used in this work in order to increase the solubility of Boltorn H*x* (**BH*x***): Brij-35, Triton X-100 and Tween-20. Non-ionic surfactants allow to minimize the effect of additional charged particles on the self-organization of hyperbranched polymers in water. These surfactants were chosen for the following reasons: firstly, the main factor of HPP self-organization in water is electrostatic interaction, secondly, these surfactants have various proportions of hydrophobic and hydrophilic molecule sections (in Brij-35 they are practically equal, in Triton-X100 (TX-100) the hydrophobic section is much smaller than the hydrophilic one, in Tween-20 the hydrophilic section is much smaller than the hydrophobic one); thirdly, such surfactants are rather low-toxic which facilitates their use in biological systems.

3.1. Self-organization and solubilization in binary systems Boltorn Hx/Brij-35

The first stage of research consisted of a study of Boltorn H*x*/Brij-35 binary systems. According to tensiometric analysis results (Fig. 2), the reduction of surface tension in BH*x*/Brij-35 systems is observed together with the increase of HPP generation, below and above the CMC point. Meanwhile, for BH30 and BH40 minimal values are observed on surface tension curves at Brij-35 concentration corresponding to the CMC point (1.7 mM). This confirms that cooperative assemblies BH*x*/Brij-35 reduce surface tension more effectively than an individual surfactant. The formation of cooperative assemblies in this system is possible when the hydrophobic portion of Brij-35 molecule penetrates the cavities between the BH*x* branches. It is known that an increase of BH*x* generation causes an increase of the branching rate, and accordingly, the number of cavities and their availability for guest molecules. Therefore, in the BH20, BH30, BH40 range the BH*x* penetration rate of surfactant molecules increases with the generation of cooperative assemblies, reaching the limit value at the CMC point (corresponding to the minimum value in Fig. 2). The increase of surface tension above the CMC point is related to system rearrangement and generation of Brij-35 micelles which dissolve BH*x* molecules.

This is confirmed by the decrease of average hydrodynamic diameter of the particles to 5–8 nm above the CMC point, which corresponds to the size of a surfactant micelle (Fig. 3). According to Fig. 2, the D_h value of cooperative assemblies BH*x*/Brij-35 (*x* = 30,

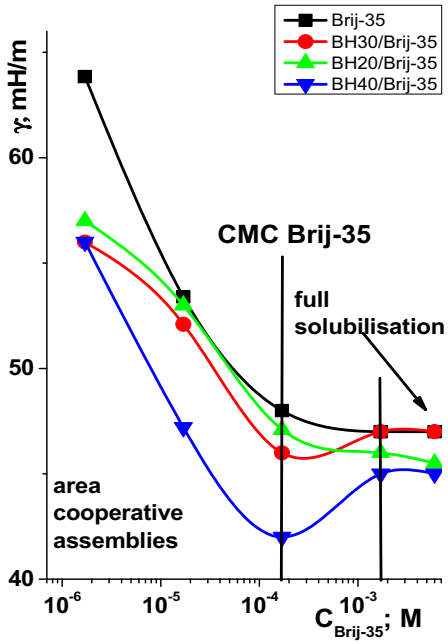

Fig. 2. Dependence of the value of surface tension in binary BH*x*/Brij-35 system on Brij-35 concentration: c(BH20) = 3.97 × 10⁻⁴ M, c(BH30) = 4 × 10⁻⁴ M, c(BH40) = 3 × 10⁻⁴ M.

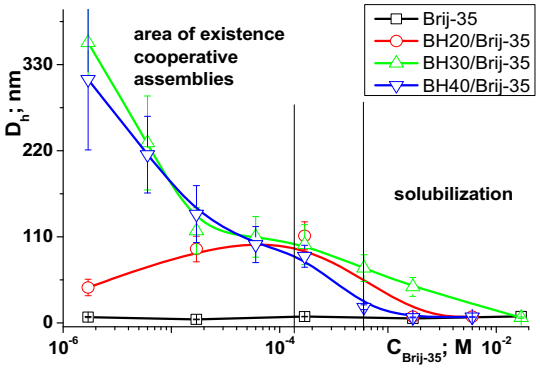

Fig. 3. Dependence of the hydrodynamic diameter (D_h) of assemblies in binary systems BH*x*/Brij-35 on the concentration of Brij-35: c(BH20) = 3.97 × 10⁻⁴ M, c(BH30) = 4 × 10⁻⁴ M, c(BH40) = 3 × 10⁻⁴ M.

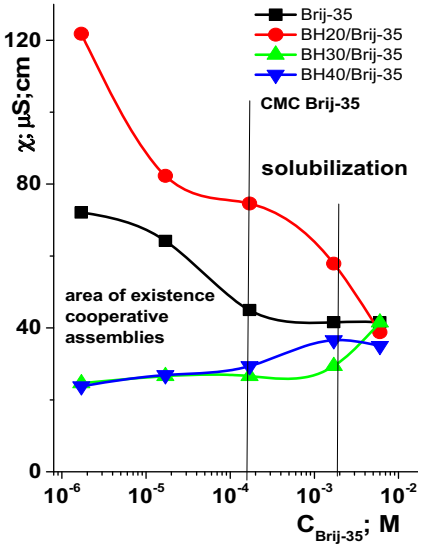

Fig. 4. Dependence of electric conductivity in BH*x*/Brij-35 binary system on Brij-35 concentration: c(BH20) = 3.97 × 10^{-4} M, c(BH30) = 4 × 10^{-4} M, c(BH40) = 3 × 10^{-4} M.

40) reduces from 320 to 90 nm with the increase of surfactant's concentration. Meanwhile, statistical dispersion of the value decreases, which clearly indicates stabilization of the system.

It can be assumed that the variation morphology of BH30/Brij-35 and BH40/Brij-35 cooperative assemblies is similar. Meanwhile, a curve with maximum D_h value at the CMC point is observed for the BH20/Brij-35 system. Presumably, the generation and structuring mechanism of BH20/Brij-35 cooperative assemblies is different from that of systems with BH30 and BH40. This assumption is confirmed by conductometric analysis (Fig. 4).

The penetration of Brij-35 in the cavities of BH30 and BH40 during the formation of cooperative assemblies leads to a quantity reduction of electrically conducting particles in the solution and an electric conductivity drop in binary systems BH*x*/Brij-35 (*x* = 30, 40) (Fig. 4). An inverse dependence is observed for system BH20Brij-35. It can be explained by the fact that during the formation of cooperative assemblies with BH20, surfactant molecules remain in the second sphere. Above the CMC point, electric conductivity in determined by surfactant's micelles with solubilized BH*x*.

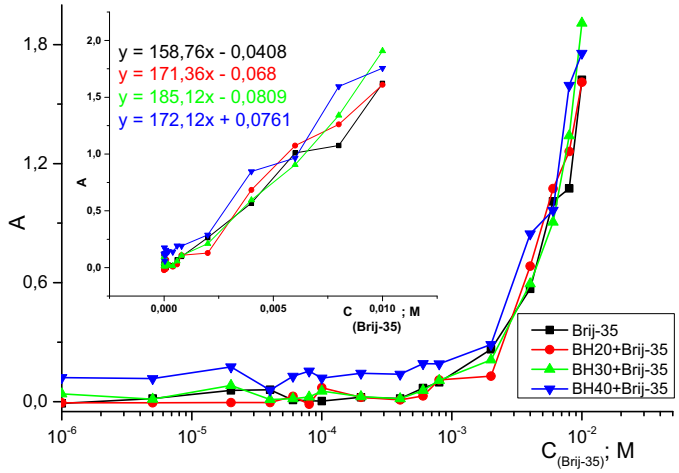

Fig. 5. Dependence of the optical density of Orange OT at λ = 505 nm in the presence of Brij-35 and in the presence of binary systems BH*x*/Brij-35: c(BH20) = 3.97 × 10^{-4} M, c(BH30) = 4 × 10^{-4} M, c(BH40) = 3 × 10^{-4} M and solubilization capacity equations.

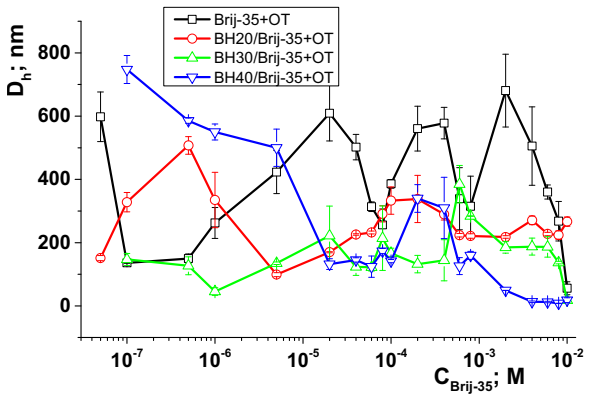

Fig. 6. Dependence of the average hydrodynamic diameter of assemblies (D_h) on the concentration of Brij-35 in binary system BH*x*/Brij-35 in the presence of Orange OT: c(BH20) = 3.97 × 10^{-4} M, c(BH30) = 4 × 10^{-4} M, c(BH40) = 3 × 10^{-4} M.

Meanwhile, the pH value of an individual surfactant solution and the pH value of the solution of BH*x*/Brij-35 systems are significantly different.

With the increase of surfactant's concentration, the pH values of the solutions shift to a single value regardless of polymer generation. Abnormally low pH value of the medium for BH*x*/Brij-35 systems can be explained by the fact that during the formation of cooperative assemblies, rearrangement of electron density occurs in the BH*x* macromolecule, facilitating its deprotonation. pH value of the BHBH20/Brij-35 binary system is different from the other values, which confirms different morphology of cooperative assemblies.

Solubilization capability of BH*x*/surfactant binary systems was evaluated at the example of standardized dye Orange-OT. Solubilization capacity of clear surfactant solution has been compared with that of its binary systems [38]. Dye solubilization in all systems is performed in a single stage and starts at concentration 4 × 10^{-4} M (Fig. 5), which correlates with the reduction of particle size in all systems in accordance with dynamic light scattering results (Fig. 6).

Meanwhile, rearrangement of assemblies occurs in clear Brij-35 at concentration 2 × 10^{-3} M, and in system BH30/Brij-35 the rearrangement point is shifted towards the increase of as surfactant concentration – 6 × 10^{-4} M (Fig. 7).

Solubilization capacity was calculated using the following formula: $S = b/\varepsilon$, where b is an absolute term of an equation of a curve (Fig. 5), and ε the molecular extinction coefficient of Orange OT, which equals to 17,400 L M^{-1} cm^{-1} [38].

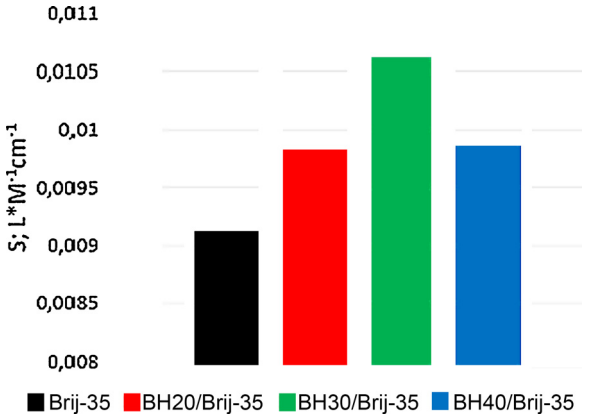

Fig. 7. Comparisons of capacity values of Orange-OT solubilization by binary systems BH*x*/Brij-35.

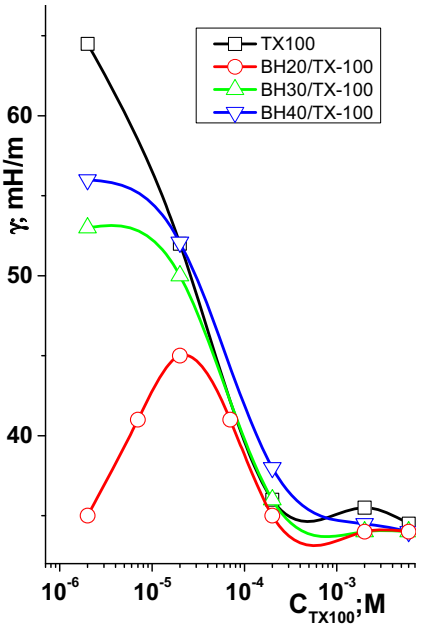

Fig. 8. Dependence of surface tension in binary systems BH*x*/TX-100 on Triton X-100 concentration: c(BH20) = 4 × 10^{-4} M, c(BH30) = 2 × 10^{-4} M, c(BH40) = 3 × 10^{-4} M.

On the basis of the equation of curve (Fig. 5), solubilization capacity was calculated for BH*x*/Brij-35 systems (Fig. 6). A significant solubilization capacity increase of Orange-OT is observed in row Brij-35 – BH20/Brij-35 – BH30/Brij-35. In system BH40/Brij-35, solubilization capacity decreases with respect to the system BH30/Brij-35. Presumably, on penetration of the Brij-35 micelle, polymer Boltorn H40 partially expels Orange OT molecules from it, reducing the system's solubilization capacity.

3.2. Self-organization and solubilization in binary systems Boltorn Hx/Triton X-100

On transition to Triton X-100 (TX-100), a difference in also observed in the variation of surface tension between systems BH*x*/surfactant (*x* = 30, 40) and BH20/surfactant. In the presence of Triton X-100, BH20 does not increase, but reduces surface tension significantly better than BH30 and BH40. On the molecular adsorption curve (Fig. 8) in system BH20/TX-100, maximum is observed at TX-100 concentration equal to 2 × 10^{-5} M, which corresponds to the CMC point. It can be assumed that in contrast to the system with Brij-35, in the presence of TX-100, BH20 develops to monomolecular micelles.

The difference in behaviour of BH30, BH40 and BH20 in binary systems with TX-100 is probable related to the fact that BH*x* structure generation three and four does not allow the hydrophobic portion of Triton-X100 molecule to remain inside the cavity formed by polymer branches. This causes instability of cooperative assemblies at low surfactant concentrations. For the BH20/TX-100 system, surface tension of the solution in areas with low surfactant concentration is 35 mN/m, which corresponds to the value of the surfactant's micelle solution. With the increase of TX100 concentration, the value of surface tension in the binary solution reaches its maximum at the surfactant's CMC point, amounting to 45 mN/m. With the increase of TX-100 concentration, rearrangement of cooperative assemblies is observed, and the surface tension value of all systems similar, which corresponds to the solubilization process of the polymer. Tensiometry results for BH*x*/TX-100 systems are confirmed by the dynamic light scattering data (Fig. 9). For hyperbranched polyester polyols BH30 and BH40, with the increase of surfactant concentration, a reduction of the average hydrodynamic diameter is observed together with a reduction of dispersion of its values, which corresponds to a rearrangement of unstable cooperative assemblies BH*x* (*x* = 30, 40)/TX-100 into micelles.

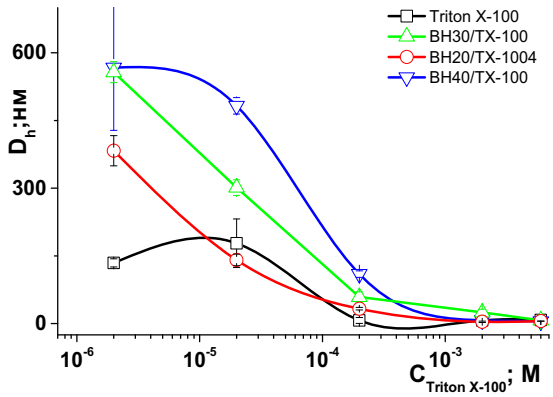

Fig. 9. Dependence of the hydrodynamic diameter of assemblies (D_h) in binary systems BH*x*/TX-100 on Triton X-100 concentration: c(BH20) = 4 × 10^{-4} M, c(BH30) = 2 × 10^{-4} M, c(BH40) = 3 × 10^{-4} M.

There are two particle types with sizes 44 and 386 nm in system BH20/TX-100 in the concentration area up to the CMC point. With the increase of TX-100 concentration, the intensity of signals with D_h = 386 nm reduces with simultaneous intensity increase of the signal with D_h = 44 nm.

The observed phenomenon can be explained by the existence of monomolecular micelles BH20 in system BH20/TX-100 at low surfactant concentrations, due to the fact that the polyester polyols in the solution possibly in the monomolecular micelles form [38]. The hydrophobic portion of TX-100 molecule can penetrate a polymer's cavity and complete a monomicelle of a hyperbranched polymer using the hydrophilic portion of the surfactant's molecule, thus increasing its solubility. This "completion" causes an effect of surfactant's concentration around the polyester polyol macromolecule with formation of assemblies with properties and morphology close to that of clear surfactant's micelles. Therefore, above the CMC point surface tension values and particle sizes in system BH20/Triton-X100 are practically the same as in other systems.

Electric conductivity of binary solutions BH*x*/TX-100 is significantly lower than that of clear surfactants (Fig. 10). This can indicate that terminal hydroxyl groups of polyester polyol are blocked by surfactant's molecules.

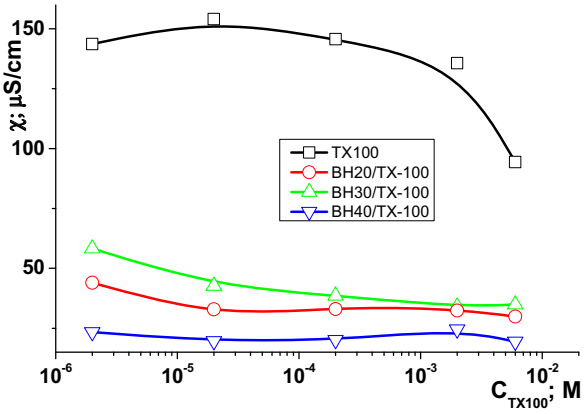

Fig. 10. Dependence of electric conductivity in binary systems BH*x*/TX-100 on Triton X-100 concentration: c(BH20) = 4 × 10^{-4} M, c(BH30) = 2 × 10^{-4} M, c(BH40) = 3 × 10^{-4} M.

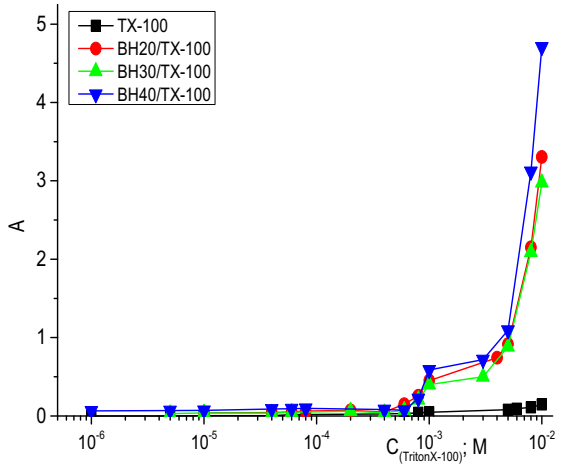

Fig. 11. Dependence of Orange OT optical density at λ = 505 nm in the presence of Triton X-100 and in the presence of binary BH*x*/TX-100 systems: c(BH20) = 3.97 × 10^{-4} M, c(BH30) = 4 × 10^{-4} M, c(BH40) = 3 × 10^{-4} M.

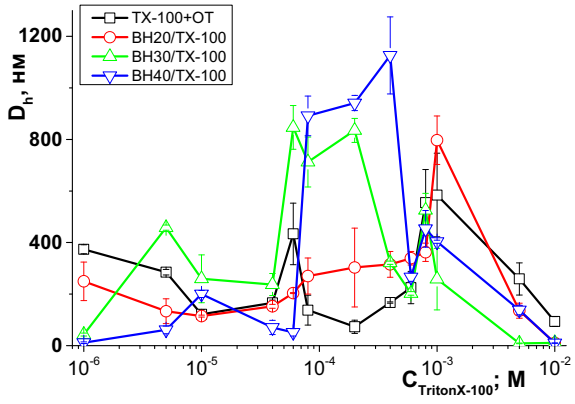

Fig. 12. Dependence of the hydrodynamic diameter of assemblies (D_h) in binary systems BH*x*/Triton X-100 in the presence of Orange OT on Triton X-100 concentration: c(BH20) = 3.97 × 10^{-4} M, c(BH30) = 4 × 10^{-4} M, c(BH40) = 3 × 10^{-4} M.

pH Values of all binary solutions BH*x*/TX-100 are higher than pH of the clear surfactant's solution. Therefore, the interaction efficiency between hyperbranched polyester polyol and Triton X-100 depends on the cavity size in polyester polyol macromolecule.

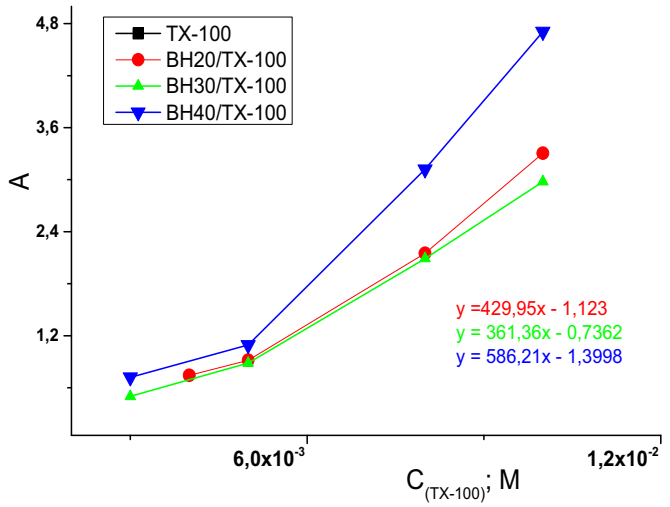

Fig. 14. Dependence of Orange OT optical density at λ = 505 nm on Triton X-100 concentration in BH*x*/TX-100 systems at the third solubilization stage: c(BH20) = 3.97 × 10^{-4} M, c(BH30) = 4 × 10^{-4} M, c(BH40) = 3 × 10^{-4} M and equations for solubilization capacity calculation.

Cavity size should correspond to the hydrophobic portion of the surfactant's molecule, which is observed for BH20.

Solubilization capacity of systems BH*x*/Triton X-100 is significantly higher than that of an individual surfactant solution (Fig. 11). Dye solubilization by BH*x*/TX-100 systems progresses in three stages.

Solubilization stages are accompanied by assemblies dimensions variation (Fig. 12).

The first solubilization stage is observed in TX-100 concentration range of 1 × 10^{-6}–2 × 10^{-4} M (Fig. 13a). The rise of cooperative assemblies size from 285 to 433 nm is observed for Triton X-100, from 133 to 302 nm for BH20/TX-100 system, from 547 to 835 nm for BH30/TX-100 system, from 61 to 941 nm from BH40/TX-100 system. It is accompanied by an increase of system dispersiveness. The second solubilization stage is observed in TX-100 concentration range 4 × 10^{-4}–1 × 10^{-3} M (Fig. 13b). In this case the minimum is observed in all systems at TX-100 concentration of 6 × 10^{-4} M, and particles are formed with the single size of D_h = 225 ± 73 nm. This suggests that at specified concentration BH*x*/Triton-X100 binary systems possess a structure, the morphology of which is

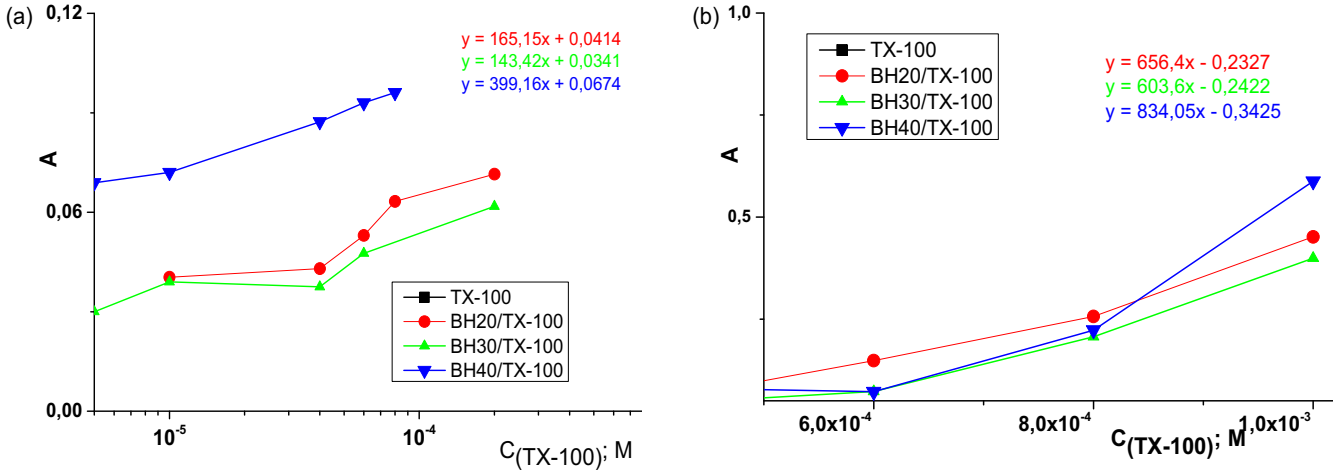

Fig. 13. (a) Dependence of Orange OT optical density at λ = 505 nm on Triton X-100 concentration in BH*x*/TX-100 systems at the first solubilization stage: c(BH20) = 3.97 × 10^{-4} M, c(BH30) = 4 × 10^{-4} M, c(BH40) = 3 × 10^{-4} M and equations for solubilization capacity calculation. (b) Dependence of Orange OT optical density at λ = 505 nm on X-100 concentration in BH*x*/TX-100 systems at the second solubilization stage: c(BH20) = 3.97 × 10^{-4} M, c(BH30) = 4 × 10^{-4} M, c(BH40) = 3 × 10^{-4} M and equations for solubilization capacity calculation.

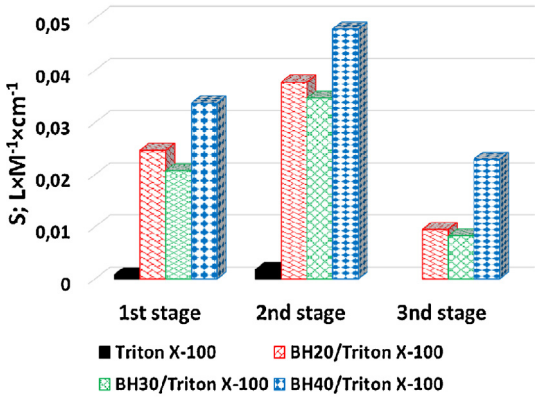

Fig. 15. Comparison of solubilization capacity values of Orange-OT by BH*x*/Triton X-100 binary systems.

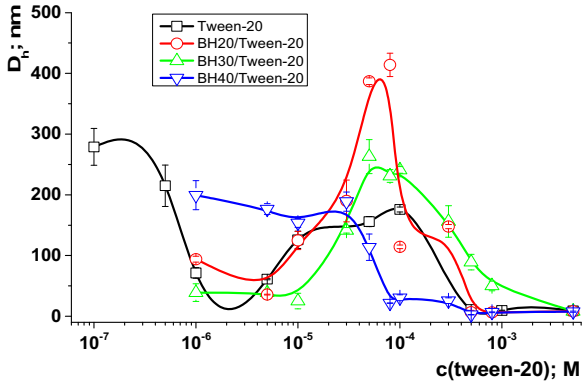

Fig. 17. Dependence of the hydrodynamic diameter of assemblies (D_h) in BH*x*/Tween-20 binary systems on Tween-20 concentration: c(BH20) = 4×10^{-4} M, c(BH30) = 2×10^{-4} M, c(BH40) = 3×10^{-4} M.

similar to Triton X-100 ordinary micelles. The similarity of systems is preserved until the second solubilization stage. At TX-100 concentration over 3×10^{-3} M, the third solubilization stage starts for binary system BH*x*/Triton X-100 (Fig. 14). At this stage particle size decreases regardless of the generation, reaching the minimum hydrodynamic diameter values of 10 ± 3 nm with simultaneous reduction of system polydispersity.

This is most probably related to the fact that dye solubilization continues in the macromolecule cavity of the hyperbranched polymer, part of complex micelle BH*x*/TX-100. It is indirectly confirmed by calculations and the solubilization capacity comparison of BH*x*/TX-100 systems (Fig. 15). Regardless of the solubilization stage, BH30/TX-100 binary system absorbs less Orange OT from the solution than binary systems based on BH20 and BH40. Thus, the hydrophobic portion of Triton X-100 molecule and Orange OT condent for a place in cavities between polymer branches. Another confirmation of this is that polydispersity is higher in the BH30/TX-100 + Orange OT system than in other binary systems.

3.3. Self-organization and solubilization in binary systems Boltorn Hx/Tween-20

The next stage of the work was studying of the BH*x*/Tween-20 binary system. According to the tensiometry data (Fig. 16), continuity of surface tension in BH*x*/Tween-20 binary systems is observed in surfactant concentration ranges from 1×10^{-8} to 1×10^{-5} M for BH20, from 1×10^{-8} to 5×10^{-6} M for BH30 and from 1×10^{-8} to 1×10^{-6} M for BH40.

For the BH20/Tween-20 system the shar change of surface tension in surfactant concentration range 1×10^{-4} M is probable due to the formation of short-lived vesicular structures which reorganize into micelles with the increase of surfactant concentration, which is indicated by the subsequent decrease of surface tension. The dynamic light scattering data (Fig. 17) confirm the formation of vesicular structures in the BH20/Tween-20 system.

Significant differences are observed between BH40/Tween-20 and BH*x*/Tween-20 systems ($x = 20$, 30). With the increase of surfactant concentration in BH20/Tween-20 and BH30/Tween-20 systems, the following step transition is observed: cooperative assembly–vesicular assembly–micelle. Direct transition from cooperative assembly to micelles is observed in the BH40/Tween-20

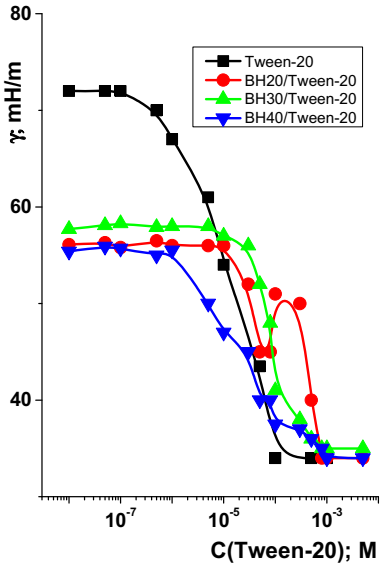

Fig. 16. Dependence of solutions surface tension in BH*x*/Tween-20 binary systems on Tween-20 concentration: c(BH20) = 4×10^{-4} M, c(BH30) = 2×10^{-4} M, c(BH40) = 3×10^{-4} M.

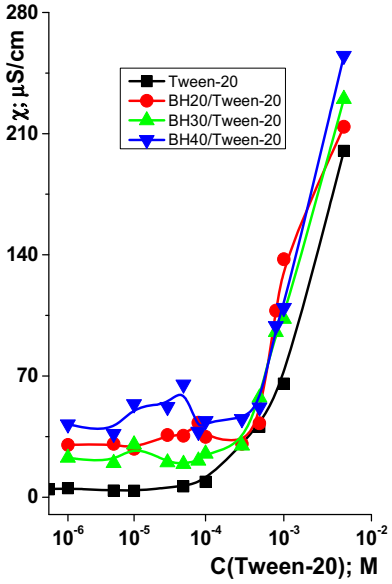

Fig. 18. Dependence of the electric conductivity of solutions in BH*x*/Tween-20 binary systems on Tween-20 concentration: c(BH20) = 4×10^{-4} M, c(BH30) = 2×10^{-4} M, c(BH40) = 3×10^{-4} M.

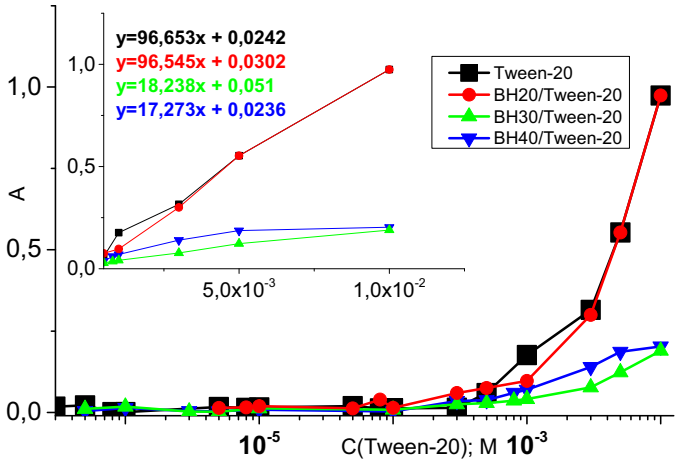

Fig. 19. Dependence of Orange OT optical density at $\lambda = 505$ nm in the presence of Tween-20 and BH*x*/Tween-20 binary systems on Tween-20 concentration: c(BH20) = 3.97×10^{-4} M, c(BH30) = 4×10^{-4} M, c(BH40) = 3×10^{-4} M and equations for solubilization capacity calculation.

system, which correlates with a more abrupt reduction of surface tension in accordance with tensiometry data (Fig. 16). It can be assumed that the generation increase of hyperbranched polyester polyol leads to stronger preorganization of Tween-20 molecules for the subsequent formation of micelles, bypassing the vesicular stage.

According to the data conductometry (Fig. 18), electric conductivity of BH*x*/Tween-20 binary systems ($x = 20$, 30) is practically matching over the entire range of surfactant concentrations.

Meanwhile in the BH40/Tween-20 system an electric conductivity increase is observed at low concentrations reaching maximum at c(Tween-20) = 5×10^{-5} M. According to pH-metry data for BH*x*/Tween-20 systems, BH*x* solubilization occurs above the CMC point of Tween-20 at surfactant's concentration of 5 mM.

Solubilization of Orange-OT by BH*x*/Tween-20 binary systems is different from that of other systems.

According to the dependency of Orange-OT optical density on the concentration of Tween-20 and its binary systems with BH20, BH30, BH40 (Fig. 19), binary systems BH30/Tween-20 and BH40/Tween-20 practically do not solubilize Orange-OT from the solution. Dependence of optical density in the BH20/Tween-20 optical system practically matches than that of the clear surfactant solution. Dependencies of particle size variation on surfactant's

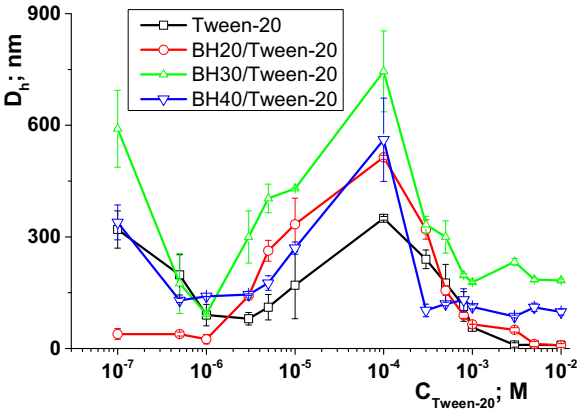

Fig. 20. Dependence of the hydrodynamic diameter of assemblies (D_h) in BH*x*/Tween-20 binary systems in the presence of Orange OT on Tween-20 concentration: c(BH20) = 3.97×10^{-4} M, c(BH30) = 4×10^{-4} M, c(BH40) = 3×10^{-4} M.

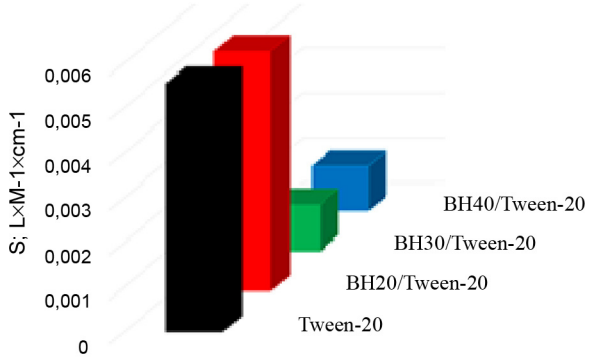

Fig. 21. Comparison of Orange-OT solubilization capacity by BH*x*/Tween binary systems depending on polymer generation.

concentration (Fig. 20) show that regardless of generation all systems undergo the same changes of assemblies' morphology. All systems have a minimum assembly size at Tween-20 concentration of 1×10^{-6} M, at which micelles formation occurs, and a maximum size at concentration 1×10^{-4} M, at which Tween-20 micelles rearrange to form vesicles. Only vesicular assemblies solubilize Orange-OT (Fig. 19); thus, hyperbranched polyester polyols generations three and four occupy practically the entire volume of vesicular bilayer, and expels dye molecules from it, whereas Boltorn H20 with smaller size does not impose competition. Presumably, it can be imposed with further dye concentration increase.

On the basis of the obtained data, solubilization capacity was obtained for systems BH*x*/Tween-20 with respect to Orange OT (Fig. 19), and a diagram for visual comparison was constructed (Fig. 21). In BH*x*/Tween-20 systems, polyester polyol BH20 does not impose strong competition on the dye. BH30/Tween-20 system solubilizes the dye slightly better than the BH40/Tween-20 system.

4. Conclusion

It can be concluded that solubilization processes of hyperbranched polyester polyols of different generations in binary systems Boltorn H*x*/surfactant (Brij-35, Triton X-100, Tween-20) are determined by hydrophobic interactions. The effectivity of hydrophobic interactions is determined by structural and dimensional correspondence between the hydrophobic cavity of the hyperbranched polyester polyol and the hydrophobic portion of the surfactant.

It has been proved that maximum solubilization capacity with respect to the standardized dye is possessed by binary systems Boltorn H*x*/surfactant, which contain surfactants with matching hydrophobic and hydrophilic portions of the molecule. Wit the dimensional increase of the hydrophobic portion of the molecule, solubilization capacity of binary systems Boltorn H*x*/surfactant decreases.

Acknowledgement

This work was funded by the subsidy allocated Kazan Federal University for the state assignment in the sphere of scientific activities (No 4.727.2014K).

Appendix A. Supplementary data

Supplementary data associated with this article can be found, in the online version, at http://dx.doi.org/10.1016/j.colsurfa.2014.11.058.

References

[1] Q. Wan, S.R. Schricker, B.M. Culbertson, Methacryloyl derivitized hyperbranched polyester. 1. Synthesis, characterization, and copolymerization, J. Macromol. Sci. A: Pure Appl. Chem. 37 (2000) 1301–1315.

[2] J. Zou, Y. Zhao, W. Shi, Encapsulation mechanism of molecular nanocarriers based on unimolecular micelle forming dendritic core–shell structural polymers, J. Phys. Chem. B 110 (2006) 2638–2642.

[3] N.S. Klimenko, A.V. Shevchuk, M.Ya. Vortman, E.G. Privalko, V.V. Shevchenko, Synthesis of hyperbranched poly(ester urethane isocyanates) and their derivatives, Polym. Sci. A 50 (2008) 160–165.

[4] P. Czech, L. Okrasa, G. Boiteux, F. Mechin, J. Ulanski, Polyurethane networks based on hyperbranched polyesters: synthesis and molecular relaxations, J. Non-Cryst. Solids 351 (2005) 2735–2741.

[5] Y. Wang, S.M. Grayson, Approaches for the preparation of non-linear amphiphilic polymers and their applications to drug delivery, Adv. Drug Deliv. Rev. 64 (2012) 852–865.

[6] R. Reul, J. Nguyen, T. Kissel, Amine-modified hyperbranched polyesters as non-toxic, biodegradable gene delivery systems, Biomaterials 30 (2009) 5815–5824.

[7] S. Chen, X.Z. Zhang, S.-X. Cheng, R. Zhuo, Z.W. Gu, Functionalized amphiphilic hyperbranched polymers for targeted drug delivery, Biomacromolecules 9 (2008) 2578–2585.

[8] F. Lasala, E. Arce, J. Otero, J. Rojo, R. Delgado, Mannosyl glycodendritic structure inhibits DC-SIGN-mediated Ebola virus infection in cis and in trans, Antimicrob. Agents Chemother. 47 (2003) 3970–3972.

[9] E. Arce, P.M. Nieto, V. Díaz, R.G. Castro, A. Bernad, J. Rojo, Glycodendritic structures based on Boltorn hyperbranched polymers and their interactions with *Lens culinaris* lectin, Bioconjug. Chem. 14 (2003) 817–823.

[10] B. Voit, New developments in hyperbranched polymers, J. Polym. Sci. A: Polym. Chem. 38 (2000) 2505–3252.

[11] C. Schüll, H. Frey, Grafting of hyperbranched polymers: from unusual complex polymer topologies to multivalent surface functionalization, Polymer 54 (21) (2013) 5443–5455.

[12] C. Sun, X. Chen, Q. Han, M. Zhou, C. Mao, Q. Zhu, J. Shen, Fabrication of glucose biosensor for whole blood based on Au/hyperbranched polyester nanoparticles multilayers by antibiofouling and self-assembly technique, Anal. Chim. Acta 776 (2013) 17–23.

[13] J. Liu, Y. Pang, W. Huang, X. Zhu, Y. Zhou, D. Yan, Self-assembly of phospholipid-analogous hyperbranched polymers nanomicelles for drug delivery, Biomaterials 31 (2010) 1334–1341.

[14] A.W. Bosman, H.M. Janssen, E.W. Meijer, About dendrimers: structure, physical properties and applications, Chem. Rev. 99 (1999) 1665–1688.

[15] M. Irfan, M. Seiler, Encapsulation using hyperbranched polymers: from research and technologies to emerging applications, Ind. Eng. Chem. Res. 49 (2010) 1169–1196.

[16] M.I. Re, Microencapsulation by spray drying, Dry. Technol. 16 (1998) 1195–1236.

[17] L.A. Tziveleka, C. Kontoyianni, Z. Sideratou, D. Tsiourvas, C.M. Paleos, Novel functional hyperbranched polyether polyols as prospective drug delivery systems, Macromol. Biosci. 6 (2006) 161.

[18] X. Huang, C.S. Brazel, On the importance and mechanisms of burst release in matrix-controlled drug delivery systems, J. Control. Release 73 (2001) 121–136.

[19] M.E. Mackay, G. Carmezini, Manipulation of hyperbranched polymers' conformation, Chem. Mater. 14 (2002) 819–825.

[20] F. Hof, S.L. Craig, C. Nuckolls, J. Rebek, Molecular encapsulation, Angew. Chem. Int. Ed. 41 (2002) 1488.

[21] D.N. Reinhoudt, M. Crego-Calama, Synthesis beyond the molecule, Science 295 (2002) 2403.

[22] Z. Shi, Y. Zhou, D. Yan, Facile fabrication of pH-responsive and size-controllable polymer vesicles from a commercially available hyperbranched polyester, Macromol. Rapid Commun. 29 (2008) 412–418.

[23] D. Wenyong, Z. Yougfeng, Y. Deyue, L. Huigin, L. Yu, pH-responsive self-assembly of carboxyl-terminated hyperbranched polymers, Phys. Chem. 9 (2007) 1255–1262.

[24] H. Hong, Y. Mai, Y. Zhou, D. Yan, Y. Chen, Synthesis and supramolecular self-assembly of thermosensitive amphiphilic star copolymers based on a hyperbranched polyether core, J. Polym. Sci. A: Polym. Chem. 46 (2008) 668–681.

[25] H. Cheng, S. Wang, J. Yang, Y. Zhou, D. Yan, Synthesis and self-assembly of amphiphilic hyperbranched polyglycerols modified with palmitoyl chloride, J. Colloid Interface Sci. 337 (2009) 278–284.

[26] G. Prevec, E. Zagar, M. Zigon, Carboxylated polyurethanes containing hyperbranched polyester soft segments, Chem. Ind. 55 (2006) 365–372.

[27] F.Kh. Karataeva, M.V. Rezepova, F.R. Yul'metov, M.P. Kutyreva, G.A. Kutyrev, Data of one-and two-dimensional NMR spectroscopy in the study of structure and nature of associations of hyperbranched polyester polyol Boltorn H20-OH, Russ. J. Gen. Chem. 80 (12) (2010) 2478–2486.

[28] W. Guo, J.Y. Park, M.O. Oh, H.W. Jeong, W.J. Cho, I. Kim, C.S. Ha, Triblock copolymer synthesis of highly ordered large-pore periodic mesoporous organosilicas with the aid of inorganic salts, Chem. Mater. 15 (2003) 2295–2298.

[29] J. Hou, G. Pan, X. Lu, C. Wei, M. Qiu, The distribution characteristics of additional extracted oil displaced by surfactant–polymer flooding and its genetic mechanisms, J. Pet. Sci. Eng. 112 (2013) 322–334.

[30] M. Ratanajanchai, D. Tanwilai, P. Sunintaboon, Visible light-induced surfactant-free emulsion polymerization using camphorquinone/tertiary amine as the initiating system for the synthesis of amine-functionalized colloidal nanoparticles, J. Colloid Interface Sci. 409 (2013) 25–31.

[31] G. Vagapova, A. Ibragimova, A. Zakharov, A. Dobrynin, I. Galkin, L. Zakharova, A. Konovalov, Novel biomimetic systems based on polyethylene glycols and amphiphilic phosphonium salt. Self-organization and solubilization of hydrophobic guest, Eur. Polym. J. 49 (5) (2013) 1031–1039.

[32] X. Cao, S. Jiang, H. Sun, X. Jiang, F. Li, Interactions of polymers and surfactants, Appl. Chem. 19 (2002) 866–869.

[33] E. Carrero, N.V. Queipo, S. Pintos, L.E. Zerpa, Global sensitivity analysis of alkali–surfactant–polymer enhanced oil recovery processes, J. Pet. Sci. Eng. 58 (2007) 30–42.

[34] M. Andersson, A. Palmqvist, K. Holmberg, W. Sigmund, H. El-Shall, B. Moudgil, D.O. Shah (Eds.), Use of Self-Assembled Surfactants for Nanomaterials Synthesis. Particulate Systems in Nano and Biotechnologies, Taylor & Francis, Inc., United Kingdom, 2009, p. 27.

[35] K. Holmberg, B. Jönsson, B. Kronberg, B. Lindman, Surfactants and Polymers in Aqueous Solution, second ed., Willey and Sons Ltd., Chichester, 2007.

[36] M.A. Voronin, D.R. Gabdrakhmanov, R.N. Khaibullin, I.Yu. Strobykina, V.E. Kataev, B.Z. Idiyatullin, D.A. Faizullin, Y.F. Zuev, L.Ya. Zakharova, A.I. Konovalov, Novel biomimetic systems based on amphiphilic compounds with a diterpenoid fragment: role of counterions in self-assembly, J. Colloid Interface Sci. 405 (2013) 125–133.

[37] E. Zagar, J. Grdadolnik, An infrared spectroscopic of H-bond network in hyperbranched polyester polyol, J. Mol. Struct. 658 (3) (2003) 143–152.

[38] K. Inoue, Functional dendrimers, hyperbranched and star polymers, Prog. Polym. Sci. 25 (2000) 453–571.